Long Term Sorption Kinetics of Phenanthrene in Aquifer Materials

HERMANN RÜGNER,
SYBILLE KLEINEIDAM, AND
PETER GRATHWOHL*

*University of Tübingen Geological Institute, Applied Geology
Group Sigwartstrasse 10, 72076 Tübingen, Germany*

Most aquifer materials are heterogeneous in terms of grain size distribution and petrography. To understand sorption kinetics, homogeneous subfractions, either separated from heterogeneous sands and gravels (lithocomponents) or fragments of fresh rocks, have to be studied. In this paper we present data on long-term sorption kinetics of phenanthrene for homogeneous samples consisting of one type of lithocomponents or fresh rock fragments in different grain sizes. Diffusion rate constants were determined in batch experiments using a numerical model for retarded intraparticle pore diffusion and correlated to grain size and intraparticle porosity of the lithocomponents. Sorption isotherms were nonlinear for all samples investigated (Kleineidam et al. (*1*)). The numerical model described the sorption kinetics very well for coarse sand and gravels. Tortuosity factors, which were obtained as final fitting factors, agreed with Archie's law predictions based on the intraparticle porosity. The dependency of sorptive uptake on grain size revealed that for smaller grains intrasorbent diffusion may become significant. This is attributed to relatively large particulate organic matter (POM) within the sedimentary rock fragments. Specifically, charcoal and coal particles, which were found in some of the sandstones, controlled the sorptive uptake rates.

Introduction

Transport of hydrophobic organic contaminants in groundwater often occurs under nonequilibrium conditions due to very slow sorption/desorption kinetics of the solutes in the aquifer material (*2, 3*) or in soils (*4*). In numerous studies it has been shown that the time required to reach sorption equilibrium or complete desorption can be months to years (*5−7*). Limiting processes are hypothesized to be the retarded diffusion in the intraparticle pore space (*7−9*) or the diffusion into the soil organic matter (OM) (*10−12*). Also, restricted diffusion in micropores may lead to slow sorption/desorption processes (*13−16*). According to Weber and Huang (*17*) and Leboeuf and Weber (*18*) condensed regions in soil organic matter with properties similar to microporous aggregates may be responsible for very slow sorption/desorption kinetics. However, since every kind of sorption site is reached via the intraparticle pores, it is in most cases not possible to distinguish between the different processes. A summary of slow sorption/desorption of organic compounds in natural particles is given by Pignatello and Xing (*19*) and Luthy et al. (*20*).

In the past intraparticle pore diffusion models have been successfully used to describe the long-term sorption kinetics in bulk samples (*7, 9, 14*). However, the tortuosity factors

obtained by such models are much higher than expected from empirical correlations based on the intraparticle porosity (*21, 22*) even within one narrow grain size fraction. It has been hypothesized that this is due to the heterogeneous composition of aquifer materials (*6, 23*). In recent investigations the sorption and desorption of contaminants in heterogeneous samples was successfully modeled using a range of (log-normal or gamma distributed) kinetic parameters (*24−27*). This approach gives good agreement with sorptive uptake in heterogeneous samples. An a priori prediction of the distribution of the rate coefficients based on independently determined properties of soil or sediment samples is still not possible.

The objective of this work was to develop empirical correlations which allow an a priori prediction of long term sorption kinetics of organic pollutants in heterogeneous sediments (aquifer materials) based on the intraparticle porosity and equilibrium sorption capacity of homogeneous constituents (lithocomponents) of the sample. Using this information, sorptive uptake and desorption in heterogeneous mixtures can be successfully predicted (*28*). Furthermore, the impact of organic matter particle size and composition on sorption kinetics was investigated (*1*) in order to elucidate the controlling diffusion mechanisms (e.g. pore diffusion vs intrasorbent diffusion).

Materials and Methods

Sampling. For the equilibrium sorption data and properties of the samples used in this study (lithocomponents from different gravel pits and the fresh rock fragments) we refer to Kleineidam et al. (*1*). A list of the samples investigated is given in Table 1. In brief, lithocomponents were separated by visual appearance from aquifer sediments of alpine origin (Hüntwangen, Singen) and from the River Neckar Valley (Horkheim) in SW − Germany. The fresh rock fragments were sampled from homogeneous strata (outcrops) in the source rock area of the River Neckar valley aquifer sediments and have therefore not experienced any changes due to weathering during transport of the sediment. For the determination of the relationship between rate constants and grain radii five different grain size fractions were used. To get the same material in each grain size fraction, the rocks were crushed, and the largest grain size (8−12.5 mm) was sieved out. A small fraction of the coarse sieve fraction was used in the kinetic experiments, the rest was broken again, and the next smaller grain size fraction (4−6.3 mm) was obtained, etc. Finally, the smallest grain size fraction was obtained by pulverization of a part of the second smallest fraction (0.125−0.25 mm) in a planet ball mill.

Sample Characterization. In addition to the organic carbon content, carbonate content and specific surface area, which are described in detail in Kleineidam et al. (*1*), the solid density (d_S), intraparticle porosity (ϵ), and pore size distribution of the samples were determined. Pores were classified according to the IUPAC (*29*): micropores: pore width < 2 nm; mesopores: 2−50 nm; and macropores: > 50 nm. Solid density was measured with a Helium pycnometer (accu pyc 1330, Micromeritics Inc., Norcross, GA). Intraparticle porosity and pore size distribution in the mesopore range was determined by nitrogen adsorption (ASAP 2010, Micromeritics). The mesopore volume was determined from the volume adsorbed up to a relative pressure of $p/p_o = 0.99$. Pore size distribution in the upper mesopore and macropore range was determined by mercury intrusion (Autopore 9220, Micromeritics). The combination of both methods, using nitrogen adsorption in the mesopore (<50 nm) and mercury

---

* Corresponding author phone: +49-(0)7071-2975429; fax: +49-(0)7071-5059; e-mail: peter.grathwohl@uni-tuebingen.de.

TABLE 1. Physical and Chemical Properties of the Lithocomponents and Rock Fragments

lithocomponents	grain size d [mm]	ϵ [−]	microporosity[c] [%]	d_S[d] [g/cm³]	dominant POM-facies[e]/ max. OM-diameter [μm]
		Hüntwangen			
dark limestone (DL$_H$)	2−4	0.0035	2.1	2.74	coal/40
dark sandstone (DS$_H$)	2−4	0.015	3.1	2.67	charcoal, coal/100
light limestone (LL$_H$)	2−4	0.011	1.2	2.73	nd
light sandstone (LS$_H$)	2−4	0.046	1.7	2.67	nd
igneous rocks (Met$_H$)	2−4	0.004	nd	2.71	nd
quartz (Qz)	2−4	0.0014	nd	2.64	nd
		Singen			
dark limestone (DL$_S$)	2−2.5/4−5	0.0034	3.1	2.70	coal, charcoal/60
dark sandstone (DS$_S$)	2−2.5/4−5	0.016	3.0	2.70	charcoal, coal/150
light limestone (LL$_S$)	2−2.5/4−5	0.0085	1.4	2.7	diverse OM/15−50
		Horkheim			
triassic limestone (MsK)	2.5−3.25	0.0070	0	2.73	nd
jurassic limestone (JK)	2.5−3.25	0.012	0	2.73	nd
triassic sandstone (SS)	2−4	0.08	<0.5	2.66	nd
bunter sandstone (BS)	2−4	0.10	<0.5	2.65	nd
		Rock Fragments			
triassic limestone (MsKr)	8−12.5/4−6.3 1−2 0.125−0.25/0.024	0.0094[a]	0	2.74	amorphous OM/5
jurassic limestone (JKr)	8−12.5/4−6.3 1−2 0.125−0.25/0.036	0.019[a]	0.9	2.71	algea, coalified wood/50
triassic sandstone (RHr)	4−6.3/1−2 0.125−0.25	0.11/0.096 0.006	0	2.65	nd

[a] ϵ of the limestone rock fragments is valid for all grain size fractions as confirmed by nitrogen adsorption. [b] Sample preparation (crushing) leads to a nearly complete loss of intraparticle porosity in case of the smallest grain size fraction of RHr; the remaining porosity was determined by nitrogen adsorption. [c] Relative amount of microporosity determined by t-plot method. [d] Standard deviations for solid density measurements <0.2%. [e] Details in Kleineidam et al. (1); nd = not determined.

intrusion in the macropore range, allowed the determination of the total intraparticle porosity over the whole range of pore sizes. This procedure avoids possible artifacts like elastic or irreversible deformation of the pore structures or compression of less rigid domains due to the high pressures (420 MPa) applied by the mercury intrusion method (30). An estimate of the micropore volume was obtained by t-plot analysis of the nitrogen adsorption isotherms. Therefore the volume adsorbed in the low-pressure region is plotted against the statistical thickness (t) of an adsorbed film of a standard isotherm (nonporous solid). The intercept on the adsorption axis of the interpolation of the data between 3.5 Å < t < 5 Å yields the micropore volume (30).

Batch Experiments. Sorption kinetics was monitored in batch experiments using phenanthrene as a representative for many hydrophobic organic chemicals. Phenanthrene is a frequent contaminant showing relatively high sorption and low volatility. The experimental setup is similar to that used for the equilibrium sorption experiments (1). Aqueous phase solutions were prepared from methanol stock solutions using deionized and degassed water at a concentration level of about 40% of the water solubility of phenanthrene. Methanol concentrations in the aqueous solution were always less than 0.5%, a level at which methanol has no measurable effect on sorption (31). Sodium azide at a concentration level of 200 mg/L was added in order to inhibit bacterial growth. The aqueous phase solutions were added to 10−50 g of the unaltered granular material consisting of narrow grain size fractions (e.g. 1−2, 2−4, and 4−6.3 mm). Prior to use the solids have been water saturated in a vacuum chamber. The batch experiments were performed in 50−100 mL crimp top reaction glass vials sealed with Teflon lined butyl rubber septa. The vials were stored at 20 °C in the dark and shaken by hand several times between each sampling interval. All experiments were carried out in triplicate. After distinct time intervals (1, 3, 7, 30, 60, 100, 250, 500, 1000 days) the aqueous phase was sampled by opening the vials and withdrawing a small aliquot (0.25−1 mL) of the supernatant water. Afterward the vials were immediately recapped using new septa.
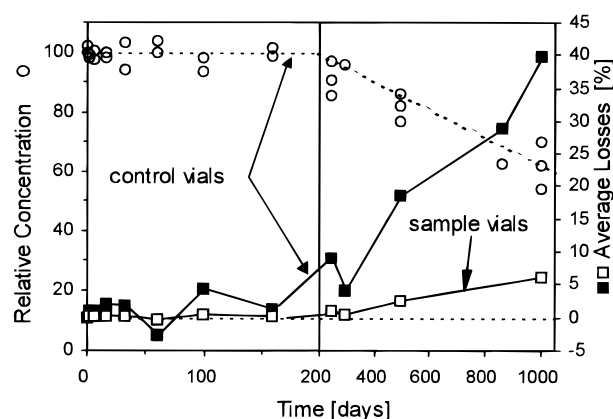

FIGURE 1. Relative concentrations in the control vials (circles) and losses during observation time. Up to 200 days no measurable loss of phenanthrene is observed in the system. At time periods up to 1000 days a linear decrease in concentration is observed presumably due to sorption/diffusion of phenanthrene into the septum. Phenanthrene losses depend on the aqueous solute concentration and are therefore much lower in the sample vials (open squares) than in control vials (filled squares), as confirmed by extraction of selected samples.

Summing up all sampling events the amount of water withdrawn was less then 10% of the initial water volume and corrected in the mass balance calculations. Phenanthrene was liquid−liquid extracted from the aqueous samples using cyclohexane and quantified using HPLC with naphthalene as an internal standard (details in 1).

The mass of phenanthrene sorbed was calculated based on the decrease of the solute concentration in the aqueous phase. Control vials containing no solids were monitored over the same time period and sampled at the same time intervals (Figure 1). Up to 200 days there was no measurable change in concentrations in the control vials, but during the next two years the concentration dropped to ca. 60% of the
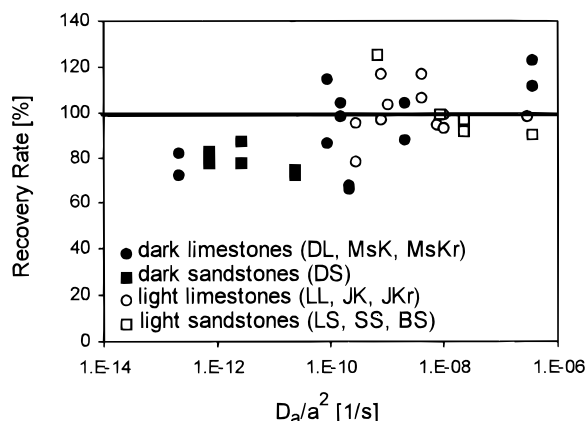
FIGURE 2. Results of the hot methanol extraction of phenanthrene from selected samples after 270−1000 days vs the diffusion rate constants measured in the sorptive uptake experiments.

initial value—this change is attributed to sorption or diffusion into the septum. Losses from the aqueous phase as observed in the control vials were accounted for in the mass balance calculations. Since losses in the vial depend on aqueous concentration, even a decrease of 40% in the aqueous concentration in the control vials results in only 5−7% overall losses in the sample vials which have much lower aqueous concentrations due to sorption to the solids (Figure 1). This was confirmed by solvent extraction of selected samples.

At the end of the observation time (270−1000 days) the solids were extracted with hot methanol (60 °C) for 3 days. The recovery rates for phenanthrene using methanol extraction were between 68 and 125% (Figure 2). The low recovery rates were mainly observed for the slow sorbing dark colored lithocomponents (high sorption capacities, large grain sizes) where 3 days may not have been sufficient for complete extraction of phenanthrene (Figure 2). Neither supercritical fluid extraction using CO_2 at 80 °C nor at increased tem-

peratures (150 °C) and addition of methanol as a modifier resulted in higher recovery rates.

Modeling of Data

Intraparticle Pore Diffusion Model. Solute diffusion from an aqueous phase into spherical aggregates can be described by Fick's second law in spherical coordinates

$$\frac{\partial C}{\partial t} = D_a \left[\frac{\partial^2 C}{\partial r^2} + \frac{2}{r} \frac{\partial C}{\partial r} \right] \quad (1)$$

where C, t, D_a, and r denote the solute concentration in the pore water [$\mu g/L$], the time [s], the apparent diffusion coefficient [cm^2/s], and the radial distance [cm] from the center of the sphere (grain), respectively. D_a/a^2 [1/s] is the diffusion rate constant where a is the grain radius [cm]. D_a in porous media (intraparticle pore diffusion) is defined as

$$D_a = \frac{D_{aq}\epsilon}{(\epsilon + K_{Fr} 1/n \, C^{(1/n-1)}\rho)\tau_f} = \frac{D_e}{\alpha} \quad (2)$$

where $(\epsilon + K_{Fr} 1/n \, C^{(1/n-1)}\rho)$ denotes the capacity factor (α). ρ, ϵ, τ_f and D_{aq} are the bulk density [g/cm^3], the intraparticle porosity [−], the tortuosity factor [−], and the aqueous diffusion coefficient [cm^2/s], respectively. D_e is the effective diffusion coefficient [cm^2/s] valid for steady-state conditions. τ_f is the only parameter in eq 2, which cannot be measured independently. Since aqueous diffusion is analogous to electrical conductivity in porous media (*32*), relationships similar to Archie's law (*33*) should predict τ_f based on ϵ alone

$$\tau_f = \epsilon^{1-m} \quad (3)$$

where m denotes an empirical exponent, which is close to 2 in sedimentary rocks. Wakao and Smith (*22*) reported a m value of 2 for diffusion of organic compounds into porous
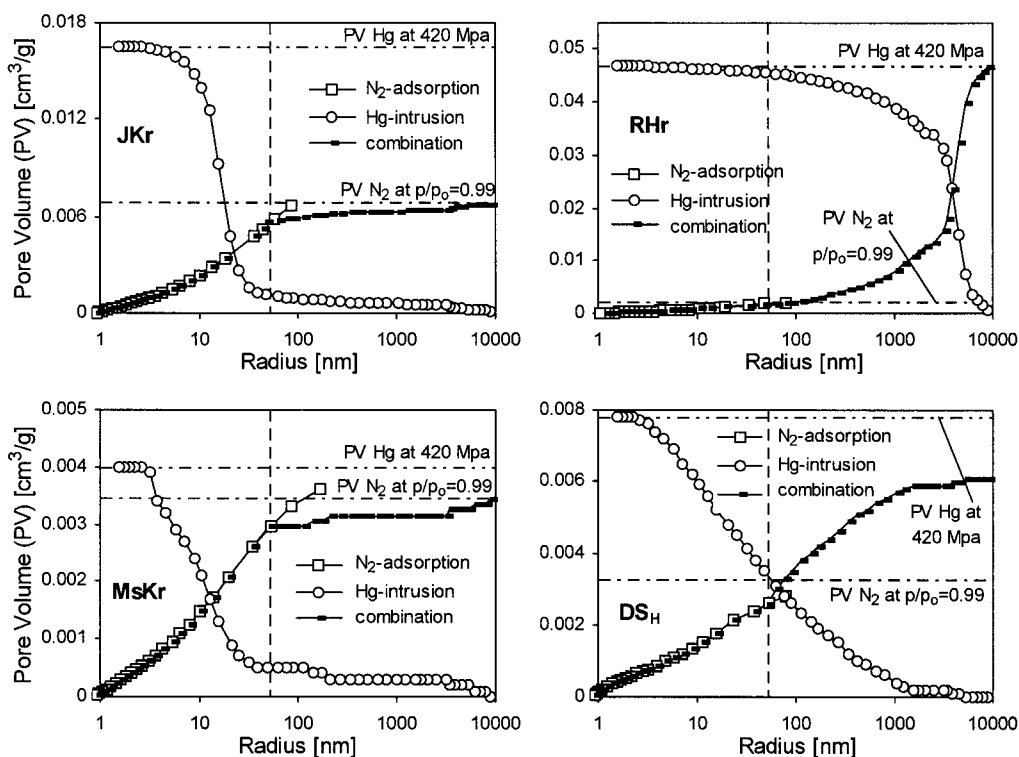

FIGURE 3. Pore size distributions from nitrogen adsorption and mercury intrusion and the combined method using N_2 in the mesopore and Hg in the macropore range of a light limestone (JKr), a light sandstone (RHr), a dark limestone (MsKr), and a dark sandstone (DS$_H$). The vertical lines mark the transition from the mesopore to the macropore range.

catalysts. Engelhard (*21*) found values between 1.8 and 2.2 for electrical conductivity in consolidated sandstones.

Analytical solutions for eq 1 are only available for linear sorption isotherms and homogeneous samples (*34*). For nonlinear sorption and heterogeneous samples a numerical model is required (*35*). The numerical model is based on the finite difference method using the Crank-Nicholson approach (implicit/explicit). Input data are the grain radius, the solid-to-water ratio, the initial water concentration, the Freundlich parameters (K_{Fr}, $1/n$), the solid density, and the intraparticle porosity. The tortuosity factor τ_f is used as final fitting parameter. If the intraparticle pore diffusion model is valid, Archie's law is expected to allow predictions of τ_f based on ϵ alone. In addition, the diffusion rate constant (D_a/a^2) is expected to increase with decreasing grain radius squared.

Results

Intraparticle Porosity and Pore Size Distribution. Nitrogen adsorption/desorption isotherms were all of Type IV (IUPAC classification, *29*) which is typical for mesoporous media. A steep increase in the volume adsorbed near $p/p_o = 1$ and the lower closure point of the hysteresis loop at $p/p_o = 0.42$ indicate that the pores may be slit shaped and macropores and micropores may be present as well. Pore size distributions for the limestones (Figure 3) show only a small amount of pore volume in the macropore range so that the intraparticle porosity can be determined from nitrogen adsorption at $p/p_o = 0.99$ alone. The sandstones have higher fractions of macropores, and a method combining N_2 adsorption and mercury intrusion was necessary to determine the overall intraparticle porosity. In both cases the Hg intrusion method overestimates the intraparticle porosity in the mesopore range presumably due to compression of the less rigid POM. This is obvious especially in the case of the light limestone JKr, where a high amount of palynomorphous POM (mostly algae) was observed in OM isolates (Table 1; Figure 3). Overall intraparticle porosities and solid densities are listed in Table 1. *t*-plot analysis of the nitrogen adsorption isotherms showed no or only minor signs for microporosity in our samples. Only the dark colored sandstones and limestones of alpine origin show a slightly higher microporous fraction (Table 1). These samples were also characterized by a low-pressure hysteresis in nitrogen adsorption/desorption isotherms (i.e. hysteresis loop does not close below $p/p_o = 0.42$) and high *C* constants (100−200) in the BET analysis (*36*). Furthermore these specific lithocomponents also contain a high amount of inertinite such as charcoals (fusinite) and highly reflecting coal particles (vitrinite) in the OM isolates (*1*) which indicates that the micropores may be located in the POM.

Sorption Kinetics—Retarded Intraparticle Pore Diffusion Model. Sorptive uptake for all lithocomponents and fresh rock fragments (Figure 4a,b) agreed very well with the numerical solutions of eq 1. The results are listed in Table 2. The quartzitic sandstones (RHr, BS), the light sandstones (SS, LS_H), and limestones (JK) showed relatively fast sorption kinetics and reached equilibrium within the observation time (<1000 days; see Figure 4a,b). The dark limestones (MsK, DL_H, DL_S) and dark sandstones (DS_H, DS_S) showed much slower sorption kinetics and were far from equilibrium even after 700−1000 days. The limestones (fresh rocks: JKr, MsKr) reached equilibrium within observation time only for grain size fractions < 2 mm. The $K_{d,eq}$ values obtained for the kinetic samples which reached equilibrium were about the same as expected from the equilibrium sorption isotherms with pulverized material (within the analytical error range). The low sorbing lithocomponents (Qz, Met_H) reached equilibrium in less than 3 days, and no modeling of the data was possible.
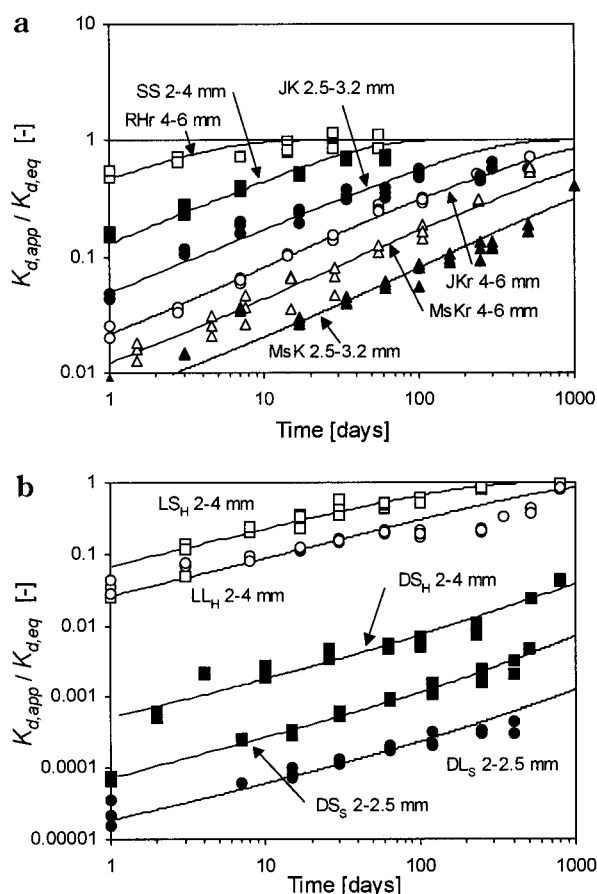
FIGURE 4. (a) Long term sorption kinetics of lithocomponents separated from the Horkheim aquifer material and fresh rock fragments (for identification of the samples see Table 1). $K_{d,app}$, nonequilibrium (apparent) K_d calculated from mass balance considerations during the sorption kinetic experiments; $K_{d,eq}$, equilibrium K_d obtained in batch experiments with pulverized samples; lines, numerical solutions of Fick's 2nd law in spherical coordinates (based on the nonlinear Freundlich type equilibrium sorption isotherms). (b) Long term sorption kinetics of some lithocomponets from the HUntwangen and Singen aquifer material (for identification of the samples see Table 1).

Discussion

Dependency of the Rate Constants of the Grain Radii. From the intraparticle pore diffusion model the diffusion rate constant (D_a/a^2) is expected to increase with decreasing grain radius squared. This was investigated by comparing phenanthrene sorption kinetics in different grain size fractions of very homogeneous fresh rock fragments. Due to nonlinear sorption D_a/a^2 depends on solute concentration, and therefore effective diffusion rate constants (D_e/a^2) were calculated (Table 2). Figure 5 shows the resulting plot of D_e/a^2 vs radius. For the limestones the dependency of the rate constants on the radius squared holds for grain size fractions larger than 0.063 mm (MsKr) and 0.5 mm (JKr). Sorptive uptake in the smaller carbonate grains is limited by a process which is 1−2 orders of magnitude slower than expected from retarded intraparticle pore diffusion in larger grains and almost independent of grain size. This process is most likely diffusion into POM present in these limestones. Photomicroscopy of OM isolates (*1*) revealed that the organic matter present in the limestones has a relatively high degree of maturity (types 2 and 3; see Kleineidam et al. (*1*)), and its particle size is only 1 order of magnitude below or in the same order of magnitude as the smallest fresh rock fragments investigated (Table 1). We therefore expect that in relatively small grains which contain relatively coarse POM (e.g. the limestone fragments)

TABLE 2. Results of the Sorption Kinetic Experiments

lithocomponents	radius[c] a [cm]	D_a/a^2 [1/s]	D_e [cm²/s]	τ_f [−]	$K_{d,eq}$ [L/kg]	error[d] [−]
Hüntwangen						
dark limestone (DL$_H$)[a]	a 0.141	4.0×10^{-11}	1.8×10^{-10}	112	79	0.378
	b 0.141	1.3×10^{-11}	9.5×10^{-11}	214	133	0.380
dark sandstone (DS$_H$)[a]	a 0.141	2.4×10^{-11}	2.2×10^{-10}	392	175	0.220
	b 0.141	3.4×10^{-12}	1.3×10^{-10}	695	706	0.118
light limestone (LL$_H$)	0.141	1.0×10^{-9}	5.4×10^{-10}	119	9.5	0.126
light sandstone (LS$_H$)	0.141	6.7×10^{-10}	1.5×10^{-9}	523	4.9	0.098
Singen						
dark limestone (DL$_S$)	0.112	3.6×10^{-14}	2.8×10^{-11}	969	16700	0.089
	0.224	1.4×10^{-14}	4.2×10^{-11}	466	17953	0.290
dark sandstone (DS$_S$)	0.112	2.7×10^{-12}	1.3×10^{-10}	709	1423	0.041
	0.224	7.1×10^{-13}	1.3×10^{-10}	696	1423	0.360
light limestone (LL$_S$)	0.224	2.9×10^{-10}	1.1×10^{-9}	46	27	0.099
Horkheim						
triassic limestone (MsK)	0.112	1.5×10^{-10}	3.0×10^{-10}	135	60	0.032
	0.141	8.5×10^{-11}	3.2×10^{-10}	127	72	0.160
jurassic limestone (JK)	0.112	7.6×10^{-9}	1.5×10^{-9}	48	5.9	0.045
	0.141	4.1×10^{-9}	1.3×10^{-9}	53	6.2	0.062
triassic sandstone (SS)	0.141	2.3×10^{-8}	7.7×10^{-9}	60	6.7	0.025
Bunter sandstone (BS)	0.141	3.6×10^{-7}	4.1×10^{-8}	14	1.9	0.160
Rock Fragments[b]						
triassic limestone (MsKr)	0.354	3.0×10^{-11}	2.1×10^{-9}	26	203	0.033
	0.178	2.1×10^{-10}	3.3×10^{-9}	17	184	0.009
	0.05	2.0×10^{-9}	2.2×10^{-9}	24	166	0.027
	0.0063	1.5×10^{-7}	1.5×10^{-9}	38	93	0.065
	0.0012	3.5×10^{-7}	3.3×10^{-10}	334	114	0.005
jurrasic limestone (JKr)	0.354	2.3×10^{-10}	4.7×10^{-9}	23	61	0.022
	0.178	7.9×10^{-10}	3.6×10^{-9}	30	55	0.015
	0.05	9.8×10^{-9}	2.7×10^{-9}	40	41	0.026
	0.0063	1.6×10^{-7}	4.8×10^{-10}	224	30	0.074
	0.0016	2.9×10^{-7}	1.4×10^{-10}	1516	37	0.015
triassic sandstone (RHr)	0.178	2.7×10^{-7}	8.8×10^{-9}	71	0.39	0.016
	0.05	5.2×10^{-7}	9.1×10^{-10}	612	0.25	0.016
	0.0063	8.0×10^{-7}	3.6×10^{-11}	974	0.43	0.075

[a] Experiments performed with different initial concentrations and solid/water ratios (fractional uptake). [b] Rock fragments: radii were reduced by a factor of 1.4 compared to the geometric means of rounded grains according to the Rosin grain size distribution of broken materials (Rosin and Rammler, (40); Kittleman, (41). [c] Geometric mean. [d] Mean weighted squared error.
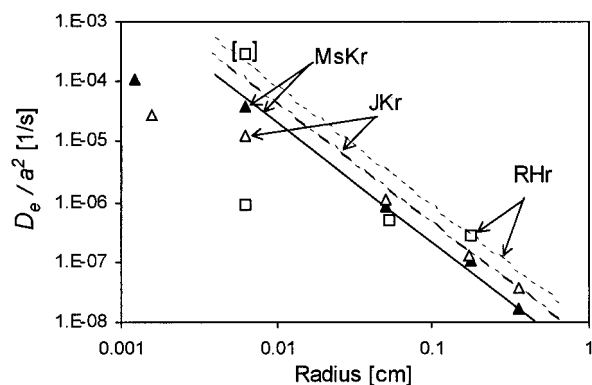

FIGURE 5. D_e/a^2 vs grain radius for fresh rock fragments of different grain size. The lines are predictions starting with the largest grain sizes. The value in brackets represents RHr (0.125−0.25 mm) assuming the same intraparticle porosity as for the larger grains.

intrasorbent diffusion (10−12) becomes the rate-limiting step in sorptive uptake.

The difference between the dark (MsKr) and the light limestones (JKr), where the dependency of the rate constants holds for grains ≥0.063 and 0.5 mm, respectively, can be explained by the type of organic matter in these sedimentary rock fragments. In the dark limestone an amorphous type of POM with a maximum particle size of 5 μm dominates, while the light limestones (JKr) have a high amount of palynomorphous POM (mostly algae and coalified wood) with a maximum particle size of 50 μm (Table 1). Whether sorptive

uptake of phenanthrene in sand and gravel sized limestone grains is governed by retarded pore diffusion or intrasorbent diffusion therefore depends mainly on the POM particle size relative to the grain size.

The diffusion rate constants determined for the light and highly porous sandstone (RHr) seem to have no correlation with the radius squared (Figure 5). Due to very low organic carbon content and log K_{OC} values (0.04 mg/g and 4.34, respectively) it seems unlikely that diffusion into mature POM could account for that behavior. However, preparing smaller and smaller grain sizes of this sandstone material resulted in a subsequent loss of porosity mainly in the macropore range (Table 1; Figure 3). Therefore it is expected that the smaller grain size fraction has a much smaller porosity and thus smaller D_e than the coarse fractions which explains the behavior observed. If we account for the loss of porosity (by an proportionally higher D_e) the data for the smallest sandstone grains would again fit the expected line (Figure 5; value in parentheses). Sorptive uptake in the smallest grain size fraction occurs presumably in dense iron and manganese hydroxide precipitates which occur in these sandstones but not in the quartz grains. These precipitates are the result of former bacterial activity and often are accompanied by organic carbon accumulation (37).

Diffusion Coefficients and Intraparticle Porosity. The diffusivity ($D' = \epsilon/\tau_f$) for the different lithocomponents and rock fragments was calculated from the measured intraparticle porosity and the tortuosity factors obtained by the numerical modeling of the sorptive uptake. D' depends only on rock properties and is therefore chemical independent assuming that the constrictivity in small micropores is
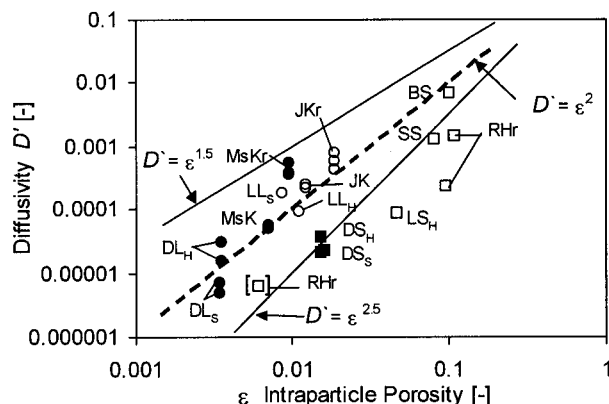
FIGURE 6. D' vs ϵ (Archie's law) for lithocomponents > 2 mm and fresh rock fragments > 1 mm (except value in brackets: RHr grain size fraction 0.125−0.25 mm).

insignificant (the mean pore size is much larger than the size of the phenanthrene molecule). Analogous to electrical conductivity in porous media (*32*) D' is expected to depend approximately on the intraparticle porosity squared. Figure 6 shows the results for the different lithocomponents ≥2 mm and rock fragments ≥1 mm investigated in this work. The limestones (MsK, MsKr, JK, JKr, DL_H, DL_S) are in very good agreement with Archie's law (*33*). Some of the light (RHr, SS, BS, LS_H) and dark sandstones (DS_H, DS_S) yield lower D' values than expected from Archie's law.

The deviation of D' from Archie's law for the alpine derived sandstones (DS_H, DS_S, LS_H) may be attributed to diffusion into POM (intrasorbent diffusion). The depositional environment of these sandstones is represented by high amounts of autochthonous palynomorphous POM with relatively large particle sizes. Furthermore the dark sandstones contain large charcoal particles (fusinite) up to 150 μm in diameter, probably produced during paleo-wildfires. These charcoals were the dominant type of organic matter in the OM isolates of these sandstones and are responsible for the high K_{OC} values observed (*1*). It is known from investigations of sediments from Lake Michigan (*38*) that carbon particles produced by anthropogenic burning of wood have typical particle sizes around 10−100 μm. This along with the relatively high intraparticle porosity (1.5−4.6%) of the sandstones could lead to limitations in sorptive uptake which is controlled by diffusion into POM also for larger grains (>2 mm).

Organic matter particles up to 60 μm in diameter (Table 1), which are dominantly coal and charcoal, and high log K_{OC} values (*1*) were also observed in the alpine derived dark limestones (DL_H, DL_S). Due to the very low intraparticle porosity and high tortuosity factors the rate constants in these sedimentary rock fragments seem to be limited by retarded intraparticle pore diffusion.

Deviations of D' from Archie's law for the highly porous sandstones separated from the River Neckar sediments and fresh rocks of the corresponding source area may be explained by slow diffusion into the low porosity matrix of these sedimentary rocks (iron and manganese precipitates which are probably associated with organic matter). Note that the smallest grain size fraction of RHr, where macroporosity was lost during sample preparation, again fits Archie's law (Figure 6; value in parentheses).

We therefore think that in most sedimentary rocks and aquifer material systems, where sorption kinetics of organic compounds is much slower than predicted by the retarded intraparticle pore diffusion model and Archie's law, this can be explained by diffusion into POM or low porosity regions inside the grains ("dual porosity" limestones/sandstones) rather than by restricted diffusion in real micropores which could also account for slow sorption processes (*13, 14, 16*).

Slow sorption and desorption processes in the condensed regions of diagenetically altered organic matter in sediments have been reported by Weber and Huang (*17*). The same authors (*17*) and Huang and Weber (*39*) reported that organic matter (condensed OM) may have properties similar to microporous sorbents where entrapment of sorbing molecules can result in sorption/desorption hysteresis. We found relatively small amounts of microporosity in the alpine derived lithocomponents investigated in this work (Table 1) presumably associated with the charcoals and highly diagenetically altered coalified wood particles in the dark sandstones and limestones. Whether this results in sorption/desorption hysteresis is investigated in ongoing research (desorption experiments).

In summary our investigations showed that the retarded pore diffusion model is valid for most of the coarse sand and gravel sized lithocomponents, and effective diffusion coefficients can be estimated based on intraparticle porosity and Archie's law (Figures 5 and 6). Sorption kinetics in this case can be predicted based on the grain size, the intraparticle porosity, and the Freundlich sorption isotherm. A comparison of the lithocomponents separated from aquifer sediments and the fresh rock fragments obtained from source rocks showed no significant impact of weathering on sorption equilibrium and kinetics.

Diffusion into POM can be the limiting mechanism in sorptive uptake in small rock fragments which contain relatively large organic matter particles (e.g. coal, charcoal) compared to the grain size. According to our observations the diffusion into the POM also follows the spherical intraparticle diffusion model (note that for porous organic matter particles the pore diffusion model probably applies again analogous to adsorption kinetics in granular activated carbons). Since the size of the POM identified in our samples is in the order of 10−150 μm (maximum diameter) relatively high sorption rate constants and therefore relatively fast equilibration is expected in POM compared to the sand and gravel sized rock fragments.

Acknowledgments

Nomenclature

a	grain radius [cm]
α	rock capacity factor [−]
C	solute concentration in pore water [μg/L]
D'	diffusivity [−]
d	grain size [mm]
D_a	apparent diffusion coefficient [cm^2/s]
D_a/a^2	diffusion rate constant [1/s]
D_{aq}	aqueous diffusion coefficient [cm^2/s]
D_e	effective diffusion coefficient [cm^2/s]
D_e/a^2	effective diffusion rate constant [1/s]
d_S	solid density [g/cm^3]
ϵ	intraparticle porosity [−]
$K_{d,app}$	apparent distribution coefficient [L/kg]
$K_{d,eq}$	equilibrium distribution coefficient [L/kg]
K_{OC}	organic carbon normalized distribution coefficient

K_{Fr}	Freundlich equilibrium coefficient [L/kg]
$1/n$	Freundlich exponent [−]
OM	organic matter
POM	particulate organic matter
p/p_o	relative pressure [−]
ρ	bulk density [g/cm³]
t	thickness of an adsorbed film [Å]; time [s]
τ_f	tortousity factor [−]

Literature Cited

(1) Kleineidam, S.; Rügner, H.; Grathwohl, P. *Environ. Sci. Technol.* **1999**, *33*, 1637−1644.

(2) Roberts, P. V.; Goltz, M. N.; Mackay, D. M. *Water Resour. Res.* **1986**, *22,* 2047−2058.

(3) Curtis, G. P.; Roberts, P. V.; Reinhard, M. *Water Resour. Res.* **1986**, *22*, 2059−2065.

(4) Pignatello, J. J.; Ferrandino, F. J.; Huang, L. Q. *Environ. Sci. Technol.* **1993**, *27*, 156−1571.

(5) Pignatello, J. J. In *Reactions and Movement of Organic Chemicals in Soils*; Sawhney, B. L., Brown, K., Eds.; SSSA: Madison, 1989; Vol. 22, pp 45−80.

(6) Ball, W. P. Ph.D. Dissertation, Stanford University, 1989.

(7) Ball, W. P.; Roberts, P. V. *Environ. Sci. Technol.* **1991**, *25*, 1237−1249.

(8) Wu, S.; Gschwend, P. M. *Environ. Sci. Technol.* **1986**, *20*, 717−725.

(9) Grathwohl, P.; Reinhard, M. *Environ. Sci. Technol.* **1993**, *27*, 2360−2366.

(10) Nkedi-Kizza, P.; Rao, P. S. C.; Hornsby, A. G. *Environ. Sci. Technol.* **1989**, *23*, 814−820.

(11) Brusseau, M. L.; Jessup, R. E.; Rao, P. S. C. *Environ. Sci. Technol.* **1990**, *24*, 727−735.

(12) Brusseau, M. L.; Jessup, R. E.; Rao, P. S. C. *Environ. Sci. Technol.* **1991**, *25*, 134−142.

(13) Farrell, J.; Reinhard, M. *Environ. Sci. Technol.* **1994**, *28*, 63−72.

(14) Harmon, T. C.; Roberts, P. V. *Environ. Sci. Technol.* **1994**, *28*, 1650−1660.

(15) Arocha, M. A.; Jackman, A. P.; McCoy, B. J. *Environ. Sci. Technol.* **1996**, *30*, 1500−1507.

(16) Werth, C. J.; Reinhard, M. *Environ. Sci. Technol.* **1997**, *31*, 697−703.

(17) Weber, W. J. Jr.; Huang, W. *Environ. Sci. Technol.* **1996**, *30*, 881−888.

(18) Leboeuf, E. J.; Weber, W. J. Jr. *Environ. Sci. Technol.* **1997**, *31*, 1697−1702.

(19) Pignatello, J. J.; Xing, B. *Environ. Sci. Technol.* **1996**, *30*, 1−11.

(20) Luthy, R. G.; Aiken, G. R.; Brusseau, M. L.; Cunningham, S. D.; Gschwend, P. M.; Pignatello, J. J.; Reinhard, M.; Traina, S. J.; Weber, W. J. Jr.; Westall, J. C. *Environ. Sci. Technol.* **1997**, *31*, 3341−3347.

(21) Engelhardt, W. v. *Der Porenraum der Sedimente*, *2. Band*; Springer-Verlag: Berlin, FRG, 1960.

(22) Wakao, N.; Smith, J. M. *Chem. Eng. Sci.* **1962**, *17*, 825−834.

(23) Schüth, Ch. Ph.D. Dissertation, University of Tübingen, FRG, 1994.

(24) Pedit, J. A.; Miller, C. T. *Environ. Sci. Technol.* **1994**, *28*, 2094−2104.

(25) Chen, W.; Wagenet, R. J. *Environ. Sci. Technol.* **1995**, *29*, 2725−2734.

(26) Haggerty, R.; Gorelick, S. M. *Water Resour. Res.* **1995**, *31*, 2383−2400.

(27) Werth, C. J.; Cunningham, J. A.; Roberts, P. V.; Reinhard, M. *Water Resour. Res.* **1997**, *33*, 2727−2740.

(28) Kleineidam, S.; Rügner, H.; Grathwohl, P. *Environ. Toxic. Chem.* In press.

(29) IUPAC *Pure Appl. Chem.* **1985**, *57*, 603−619.

(30) Gregg, S. J.; Sing, K. S. W. *Adsorption, surface area and porosity*, 2nd ed.; Academic Press Inc.: London, U.K., 1982.

(31) Nkedi-Kizza, P.; Rao, P. S. C.; Hornsby, A. G. *Environ. Sci. Technol.* **1987**, *21*, 1107−1111.

(32) Klinkenberg, I. J. *Geol. Soc. Am. Bull.* **1951**, *62*, 559−563.

(33) Archie, G. E. *Trans. A. I. M. E.* **1942**, *146*, 54−61.

(34) Crank, J. *The mathematics of diffusion*; 2nd ed.; University Press: Oxford, U.K., 1975.

(35) Jäger, R.; Liedl, R. *Grundwasser* Submitted for publication.

(36) Brunauer, S.; Emmet, P. H.; Teller, E. *J. Am. Chem. Soc.* **1938**, *60*, 309−319.

(37) Lovley, D. R. *Microbiological Rev.* **1991**, *55*, 259−287.

(38) Karls, J. F.; Christensen, E. R. *Environ. Sci. Technol.* **1998**, *32*, 225−231.

(39) Huang, W.; Weber, W. J. Jr. *Environ. Sci. Technol.* **1997**, *31*, 2562−2569.

(40) Rosin, P.; Rammler, E. *Kolloid Zeitschrift* **1934**, *67*, 16−26.

(41) Kittleman, L. R., Jr. *J. Sedim. Petrol.* **1964**, *34*, 483−502.